10th World Congress on Structural and Multidisciplinary Optimization
May 19 - 24, 2013, Orlando, Florida, USA

h-Adaptive Extended Finite Element Method for Structural Optimization

Xuefeng Tian, Michael Yu Wang

Department of Mechanical and Automation Engineering, The Chinese University of Hong Kong, Shatin, NT, Hong Kong, yuwang@mae.cuhk.edu.hk

1. Abstract
This paper introduces h-Adaptive eXtended Finite Element Method (X-FEM) which is used for level set based structural optimization. Compared to X-FEM with uniform meshes, meshes of h-adaptive X-FEM are adequately adjusted so that meshes of higher resolution at the vicinity of the structural boundaries while meshes of relatively lower resolution in the regions far away from boundaries are adopted to improve the efficiency on the one hand and make sure the accuracy on the other hand. Elements with hanging nodes are produced while generating adaptive meshes which is restrained to 1-irregular meshes. The hanging nodes are treated with degrees of freedoms (DOFs) by modifying shape functions of elements. In addition, the imposition of boundary conditions including Neumann and Dirichlet boundary conditions are investigated. Numerical examples are conducted to verify the proposed X-FEM for structural optimization.
2. Keywords: X-FEM, adaptive, level set, structural optimization, boundary conditions, hanging nodes

3. Introduction

Belytchko *et al* [1] first introduced X-FEM into the level set based structural optimization. The X-FEM associated with the level set description of structure is an elegant combination which provides an efficient and flexible treatment of problems involving moving boundaries. On the one hand, the level set method provides a capability of description of arbitrary smooth boundaries and handling topological changes naturally. On the other hand, the level set based structural optimization method benefits from the fixed meshes using X-FEM to prevent from suffering mesh management trouble. Further research works have been conducted during the past few years.

The combination of X-FEM and level set was applied to generalized shape optimization by Duysinx *et al* [2] for 2D problems, which was later extended to 3D and stress concentration optimization by [3, 4, 5]. A nodal based two-phase material topology optimization using X-FEM and level set description wea proposed by Lee *et al* [6], in which design variables are nodal densities and material properties are assumed as Gauss quadrature point densities. Wei *et al* [7] investigated the X-FEM for continuum structural optimization with level set description and proposed a partition method to deal with numerical integral of cut elements of 2D. Li in her PhD thesis [8] studied numerical issues of X-FEM including both efficiency and accuracy aspects for level set based structural optimization. The X-FEM was also incorporated with level set description in PhD thesis of Miegroet [9].

The X-FEM associated with level set method is a perfect combination which shows a promising potential to balance both accuracy and efficiency in structural optimization. Even though much effort has been made, there are still space to improve. In level set based structural optimization, boundaries are most concerned. The level set method provides the capability of finding precision boundaries, which contributes to improve the accuracy of the X-FEM. Therefore, the denser meshes are, the more precision boundaries are achieved. Nevertheless, fixed uniform are usually employed leading to increasing the resolution of meshes would dramatically decrease the efficiency of the X-FEM. The motivation of this paper is to find out a balance between efficiency and accuracy of the X-FEM.

To overcome the difficulty, h-Adaptive X-FEM is proposed, in which higher resolution of finite element meshes in the vicinity of the boundaries and relatively lower resolution in the regions away from boundaries are adopted resulting in a significant decreasing of computing time cost while ensuring the accuracy.

4. Implementation of h-Adaptive X-FEM

4.1. X-FEM for material-void interfaces

Typically, the discontinuities in the structure can be classified as two categories: strong and weak dis-

continuities. The weak discontinuities appear in the high gradient regions, such as interfaces between two different materials, as the forms of kinks in analysis solution. In contrast, strong discontinuities are present at the vicinity of cracks or material-void interfaces as the forms of discontinuities in analysis solution. In the study, we concern on the X-FEM for level set based structural optimization, where strong discontinuities, i.e., material-void interfaces happen.
As suggested in [10] and [11], material-void strong discontinuities are modelled with a Heaviside function as:

$$u^h(x) = \sum_{i \in I} N_i(x) H(\Phi(x)) u_i \tag{1}$$

where $\Phi(x)$ is the level value at nodal point and the Heaviside function is defined as:

$$H(\Phi(x)) = \begin{cases} 1, & if \quad \Phi(x) \geqslant 0 \\ 0, & if \quad \Phi(x) < 0 \end{cases} \tag{2}$$

Actually, in practical implementation, the Heaviside function $H(\Phi(x))$ is not really introduced and for the cut elements the element stiffness is only computed in the solid part whereas the void elements are directly removed from the system. Therefore, the benefit of modeling material-void interfaces with X-FEM is no additional degree of freedoms are introduced to the system, which is a perfect choice for the level set based structural optimization.

4.2. Implementation of adaptive meshes

As mentioned above, fixed uniform meshes are typically employed in X-FEM for structural optimization. To capture more precision boundaries, denser meshes are necessary, which to some extent increases computational cost. Therefore, the intention of this study is to implement adaptive meshes instead of uniform meshes to alleviate this issue. To achieve adaptive meshes, there are two opposite ways: mesh refinement or mesh coarsening.

For the mesh refinement, adaptive meshes are built by dividing coarse meshes recursively until satisfying the requirement, and the level set values for newly created nodal points are interpolated based on coarse meshes. However, the level set function defined on the coarse meshes is not sufficient to construct the adaptive mesh because the boundaries represented by a level set function which is defined on coarse meshes are initially inaccurate, leading to boundaries depicted by the final adaptive meshes are inaccurate as well.

However, opposite to mesh refinement, mesh coarsening is a procedure to remove unnecessary elements from initial fine uniform meshes to achieve adaptive meshes. The level set function defined on the fine meshes is accurate enough to represent boundaries of structure. Therefore, the boundaries reconstructed by adaptive meshes are the same accurate as the ones constructed by initial fine meshes because only element removing operations are carried out with no interpolation, and the resolution of meshes in the vicinity of boundaries are equivalent to the resolution of fine meshes. Compared to these two procedures, mesh coarsening is better and implemented in the study.

4.3. 1-irregular meshes

Different from mesh refinement in conventional FEM, the adaptive meshes used for X-FEM are not necessarily conforming to boundaries of structure, resulting in irregular meshes which contain so called hanging nodes. However, it was pointed out in [12, 13] that conforming mesh refinement in conventional FEM is more complex than generation of these irregular meshes with hanging nodes, in particular for 3D problems. Hanging nodes refer to those which not only appear in element corners, but also on element edges or faces of their neighbouring elements. In this paper, adaptive meshes are restrained to 1-irregular meshes [14], in which, hanging nodes are only present in the center of element edges (2D) and center of edges and faces (3D). Not like Fries *et al* [15] where hanging nodes are also enriched for the consideration of specific applications, only standard elements without hanging nodes are enriched. Therefore, elements with hanging nodes are never cut by boundaries of structure. Depending on whether DOFs are associated with hanging nodes, there are two approaches to deal with hanging nodes. No matter which method is adopted, the requirement that shape functions of each element build a partition of unity should be satisfied.

In case of DOFs are associate with hanging nodes, corresponding shape functions should be attached to these hanging nodes. Shape functions suggested by Gupta [16] for 2D and Morton *et al* [17] for 3D satisfy the partition of unity requirement and are implemented here for its simplicity. For the elements without hanging nodes, standard shape functions and enrichment functions are considered to compute

element stiffness. Special treatment is taken while dealing with elements with hanging nodes.

4.4. Refinement Criteria

The structural model is implicitly represented by level set function, and boundaries are clearly captured. For the discretized domain, level set value for each nodal point is known. Based on these information, *a priori* threshold on level set values is proposed to realize adaptive meshes. Elements which lie completely within the threshold remain in the meshes, otherwise deleted. The condition is expressed as:

$$Adap = \{e : \max |\Phi(x)| < threshold\} \tag{3}$$

where e stands for element, $\Phi(x)$ is the level set value for nodal point. If the maximum of absolute values of all the nodes is less than the *threshold*, *Adap* indicates the element should still remain in the meshes. In practical implementation, the *threshold* is set as:

$$threshold = n \bullet s_f \tag{4}$$

where s_f is the size of finest mesh, n is an integer, which indicates the number of fine meshes around boundaries. For example, a 2D plane model with holes in Figure (1a) is first discretized by uniform meshes in Figure (1b), and then adaptive meshes are generated with $threshold = 3 \bullet s_f$ as shown in Figure (1c).

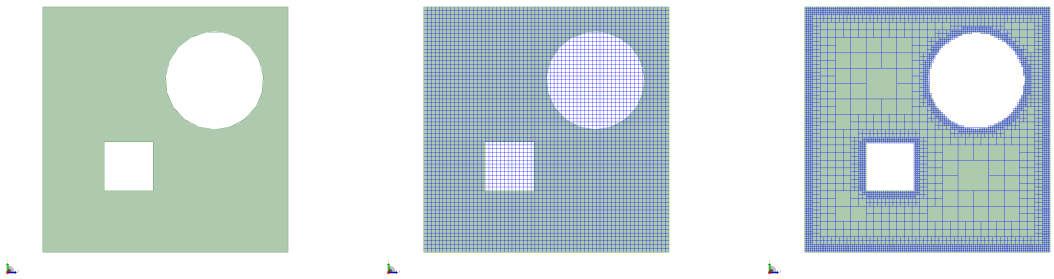

(a) 2D model (b) Uniform meshes (c) Adaptive meshes

Figure 1: A 2D plane model with holes (a) is discretized by (b) uniform mesh and (c) adaptive meshes with $threshold = 3 \bullet s_f$ respectively

4.5. Quadrature for elements with hanging nodes

Similar to regular nodes, the hanging nodes herein are treated with DOFs. Therefore, the corresponding shape functions are assigned to the hanging nodes. In each element with hanging nodes, the shape functions need to build a partition of unity. Only 2D cases are studied in this paper and standard bilinear quadrilateral elements (Q4) are employed.

Shape functions for 1-irregular meshes of 2D employed in this study were proposed by Gupta in [16]. In Figure (2), a Q4 element defined in reference space (ξ, η) with 4 regular nodes (in black) and 4 hanging nodes (in blue) on centers of the element edges. The shape functions defined on the hanging nodes are given as:

$$N_5^* = \frac{1}{2}(1 - |\xi|) \cdot (1 - \eta) \tag{5}$$

$$N_6^* = \frac{1}{2}(1 + \xi) \cdot (1 - |\eta|) \tag{6}$$

$$N_7^* = \frac{1}{2}(1 - |\xi|) \cdot (1 + \eta) \tag{7}$$

$$N_8^* = \frac{1}{2}(1 - \xi) \cdot (1 - |\eta|) \tag{8}$$

It is not necessary all these four hanging nodes must be present at the same time in one element. If any of the hanging nodes is not present in its position, the corresponding shape function is set to zero.

To satisfy the partition of unity property, the shape functions for the regular nodes are modified as:

$$N_1^* = \frac{1}{4}(1-\xi)\cdot(1-\eta) - \frac{1}{2}(N_5^* + N_8^*) \tag{9}$$

$$N_2^* = \frac{1}{4}(1+\xi)\cdot(1-\eta) - \frac{1}{2}(N_5^* + N_6^*) \tag{10}$$

$$N_3^* = \frac{1}{4}(1+\xi)\cdot(1+\eta) - \frac{1}{2}(N_6^* + N_7^*) \tag{11}$$

$$N_4^* = \frac{1}{4}(1-\xi)\cdot(1+\eta) - \frac{1}{2}(N_7^* + N_8^*) \tag{12}$$

It is noted that the shape functions build a partition of unity over the element. However, the shape functions are not continuous through the whole element domain because kinks are present at the positions of hanging nodes. To solve this issue, a special quadrature scheme is desired in the elements with hanging nodes. The element domain is divided into 4 sub-cells. Then 4 Gauss points are located in each sub-cell and in total there are 16 Gauss points for a Q4 element with hanging nodes, see Figure (3).

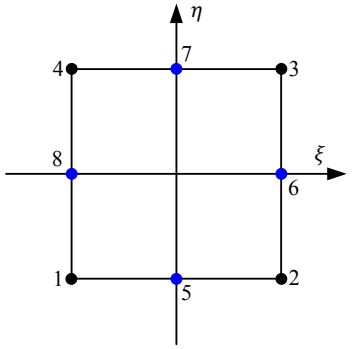

Figure 2: Q4 element in reference space (ξ, η) with hanging nodes

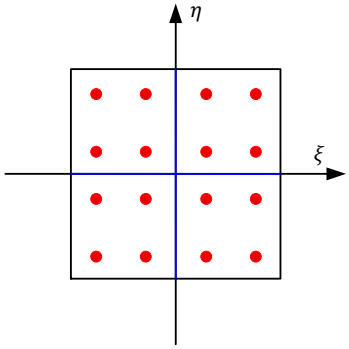

Figure 3: Gauss points (in red) for a Q4 element with hanging nodes

4.6. Imposition of boundary conditions

Not like conventional FEM, meshes in X-FEM are not necessarily conforming to the structural boundaries, which brings difficulties to impose boundary conditions. Imposition of Neumann boundary conditions is quite straightforward since it only requires to modify distribution of loads to all the nodes of the elements crossed by Neumann boundaries. In contrast, imposing Dirichlet boundary conditions is non-trivial as the K-δ property is not satisfied.

4.6.1 Imposition of Neumann Boundary Conditions

Using FEM for linear static problems, if the body forces are ignored, the external loads are expressed as:

$$\vec{f}_i = \int_{\Gamma_t^h} \vec{t} \cdot N_i(x)\, d\Gamma \tag{13}$$

where $\vec{t}$ is the load vector and Γ_t^h is the discretization of boundary Γ_t. In the conventional FEM, the boundary coincides with FE meshes so that the Equation (13) is always conducted along the edges or faces of the elements. Therefore, the load vectors are only distributed to the nodes belonging to edges or faces of the elements where the Neumann boundary conditions are applied. However, the situation is different in X-FEM as the meshes may not conforming to the boundary Γ_t^h which can lie inside the meshes. The Equation (13) still holds but the integral domain changes to the boundary inside the element from the borders of the elements. Therefore, the load vectors are distributed to all the nodes of the elements where the Neumann boundary conditions are prescribed. The comparisons of Neumann boundary conditions between FEM and X-FEM are shown in Figure (4) for 2D, the red edge or face represents the Neumann boundaries and load vectors are distributed to red nodes.

4.6.2 Imposition of Dirichlet Boundary Conditions

It is difficult to impose Dirichlet boundary conditions in X-FEM as the meshes are not necessarily conforming to the structural boundaries, which means the Dirichlet boundary can lie inside the meshes. Typically, three types of approaches are employed to solve this issue: (1) Penalty method; (2) Augmented Lagrange multiplier method; (3) Nitsche's method.

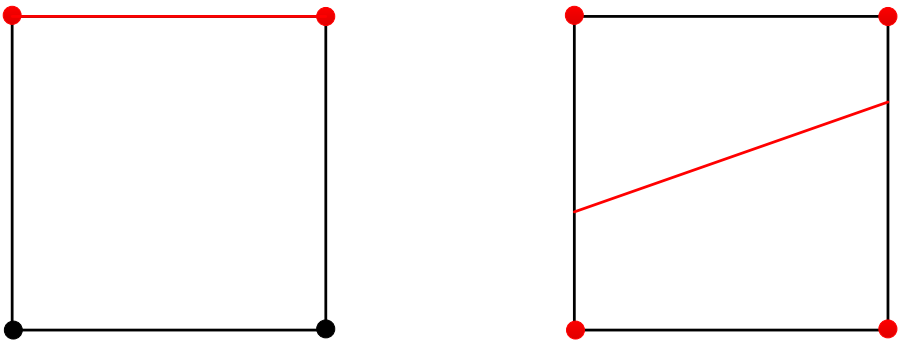

(a) FEM (b) X-FEM

Figure 4: Comparison of load vector distributions between FEM and X-FEM in 2D

In this paper, Nitsche's method [18] is used to enforce Dirichlet boundary conditions. The idea behind Nitsches method is to simply replace the Lagrange multipliers arising in a dual formulation through their physical representation, namely the normal flux at the interface. The Nitsche's method also adds an additional penalty like term to ensure the coercivity and the positive definiteness of the bilinear form. The one-variational formulation of Nitsche's method in term of energy form is given as:

$$\begin{aligned}\Pi^p(u) =& \Pi(u) + \int_{\Gamma_D} (u-u_0)\cdot\sigma(u)\cdot\vec{n}d\Gamma \\ &+ \frac{1}{2}\beta\int_{\Gamma_D}(u-u_0)^T(u-u_0)\,d\Gamma\end{aligned} \tag{14}$$

where $\sigma(u)$ is the stress vector for linear static problems and $\vec{n}$ is defined as the normal vector.

The discretization for field approximation can be written in matrix form to obtain a linear system:

$$(K_b - K_n + K_s)\,U = f_b - f_n + f_s \tag{15}$$

where U is the displacement field, K_b are f_b are stiffness matrix and force vector of the original system respectively, which are defined as:

$$K_b = \int_{\Omega^h} B^T D B d\Omega \tag{16}$$

$$f_b = \int_{\Gamma_N^h} N^T f d\Gamma \tag{17}$$

where N is the shape functions, Ω^h is the structural domain and Γ_N^h is the Neumann boundaries.

The other four terms are defined as:

$$K_n = \int_{\Gamma_D^h} N^T D B\cdot\vec{n}d\Gamma + \int_{\Gamma_D^h} B^T D^T N\cdot\vec{n}d\Gamma \tag{18}$$

$$K_s = \int_{\Gamma_D^h} \alpha N^T N d\Gamma d\Gamma \tag{19}$$

$$f_n = \int_{\Gamma_D^h} B^T D^T u_0\cdot\vec{n}d\Gamma \tag{20}$$

$$f_s = \alpha\int_{\Gamma_D^h} N^T u_0 d\Gamma \tag{21}$$

where Γ_D^h is the Dirichlet boundaries.

The Nitsche's method is employed in this study to impose Dirichlet boundary conditions because of the following reasons:

- No additional unknowns are introduce into the system so that the DOFs of the linear system remains the same as the original one;

- The stability parameter ensures the positive definiteness of the linear system;
- From an implementation perspective, Nitsche's method is clearly less intrusive in standard codes as all the modifications arise at an element level.

5. Numerical Examples

In this section, a numerical example is used to validate the proposed X-FEM including imposition of boundary conditions, accuracy, efficiency and convergent rate. Another example is to verify the proposed X-FEM applied to level set based structural optimization.

5.1 A Thick Cylinder Model Under Internal Pressure

As shown in Figure (5a), a hollow walled cylinder of internal radius $a = 0.6m$ and external radius $b = 1.0$ under internal pressure $P = 1MPa$ along radial direction is modeled. Only a quarter of the cylinder shown in Figure (5b) is chosen for analysis due to property of symmetry. The material is assumed to be steel with Young's modulus $E = 200GPa$ and Poisson's ratio $\nu = 0.3$. The Dirichlet boundary condition are imposed on the left and bottom edges of the quarter resulting in radial displacement is allowed while the tangential displacement is restricted. From [**?**], the analytical solution of displacement and stresses as a function of radial position r is given as:

$$u_r = \frac{r}{E\left(b^2 - a^2\right)}\left[\left(1-\nu\right)pa^2 + \frac{\left(1+\nu\right)pa^2b^2}{r^2}\right] \tag{22}$$

$$\sigma_{rr} = \frac{pa^2\left(r^2 - b^2\right)}{r^2\left(b^2 - a^2\right)} \tag{23}$$

$$\sigma_{\theta\theta} = \frac{pa^2\left(r^2 + b^2\right)}{r^2\left(b^2 - a^2\right)} \tag{24}$$

The mesh model of the cylinder is shown in Figure (5c), which is obviously not conforming to the boundaries because the Q4 elements can not exactly match the circular arcs. Therefore, the Neumann boundary of internal circular arc lies inside the elements. The distributions of radial displacement field u_r, radial stress σ_{rr} and tangential stress $\sigma_{\theta\theta}$ are illustrated in Figure (6), which apparently demonstrates that the distributions of stresses are radial as the Equation (23) and (24) show.

The comparison of efficiency with the same model of uniform meshes is listed in Table (1).

Table 1: Comparison of efficiency with cylinder model of uniform meshes

Item	Quadtree Depth	Threshold	Elements	Nodes	Time(s)
h-Adaptive	9	10	8910	9855	12.596
Uniform	9	> 256	33303	33816	28.338

In order to further verify the accuracy, the comparisons of u_r, σ_{rr} and $\sigma_{\theta\theta}$ between the proposed X-FEM and analytical solution are investigated along the line of $\theta = \pi/4$, which are shown in Figure (7), which obviously validate the accuracy of the proposed X-FEM.The convergent rates of L_2 error norm and energy error norm are illustrated in Figure (8).

5.2 h-Adaptive X-FEM for level set based structural optimization

In this section, the proposed X-FEM is used for level set based structural optimization to further verify its accuracy and efficiency. The objective is set as mean compliance of structure and the constraint is volume constraint as 0.5. The shape sensitivity analysis can be found in [19]. A cantilever beam with a length and width ratio of $L : H = 2 : 1$, which is subjected to a concentrated load of $F = 1$ at the center of right edge while the left edge is fixed as shown in Figure (9). It is assumed that Young's modulus is equal to 1 and the Poisson's ratio is 0.3. In order to demonstrate the efficiency of the proposed X-FEM, the optimization is conducted based on uniform and adaptive meshes separately. For the optimization with uniform meshes, the design domain is discretized by 128×64 elements, while for the optimization with adaptive meshes, the adaptive threshold is set as $3 \cdot n_f$ and the size of the finest elements is the same to the size of elements of uniform meshes. intermediate results for optimizations of uniform and adaptive meshes are illustrated in Figure (10) and (11) respectively. It clearly shows that the difference of final results. The comparison of efficiency is listed in Table (2), which obviously shows that the time

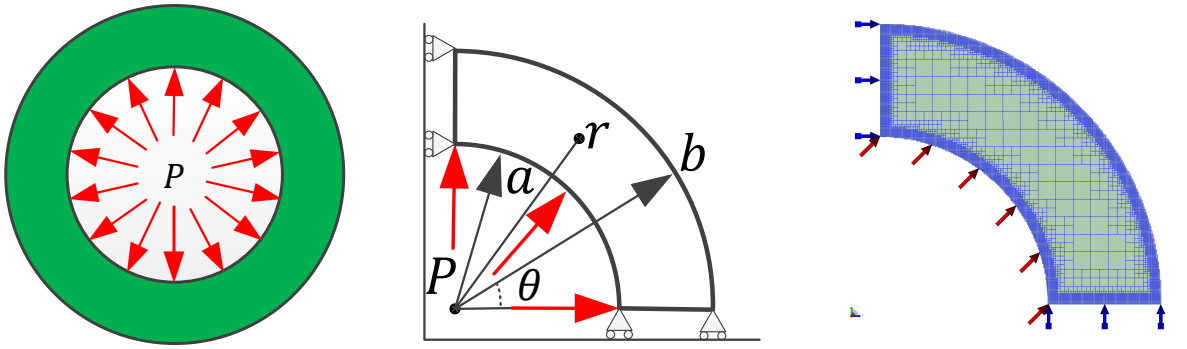

(a) A full thick cylinder model (b) A Quater of the thick cylinder model (c) The mesh model of the cylinder

Figure 5: A plate model under uniaxial tension

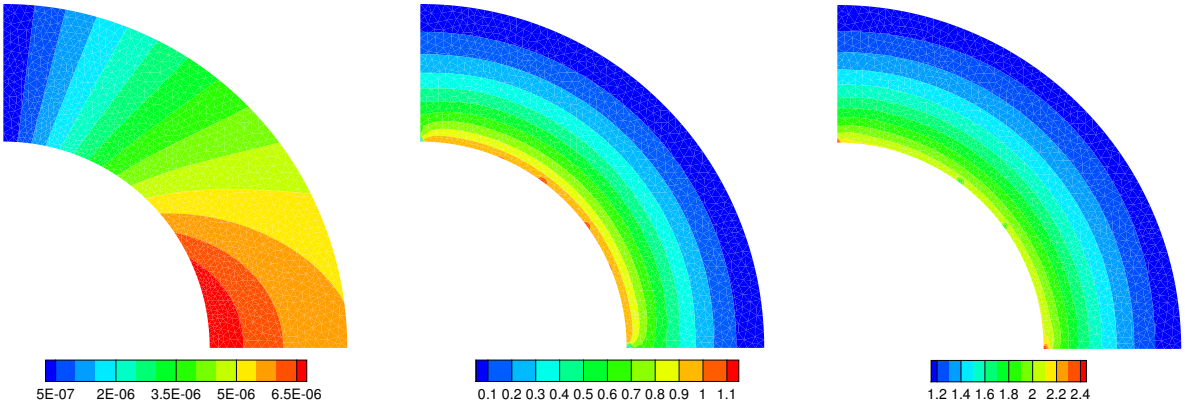

(a) u_r (b) σ_{rr} (c) $\sigma_{\theta\theta}$

Figure 6: Contour plot of u_r, σ_{rr},$\sigma_{\theta\theta}$

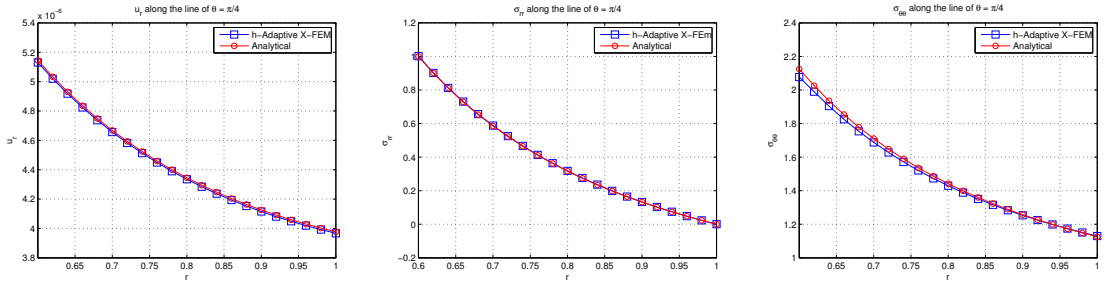

(a) Comparison of u_r (b) Comparison of σ_{rr} (c) Comparison of $\sigma_{\theta\theta}$

Figure 7: Comparisons of u_r, σ_{rr} and $\sigma_{\theta\theta}$ between the proposed X-FEM and analytical solution

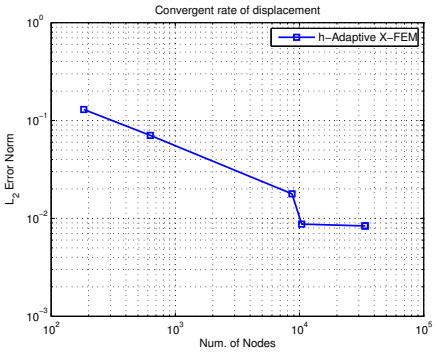

(a) Convergent rate of displacement

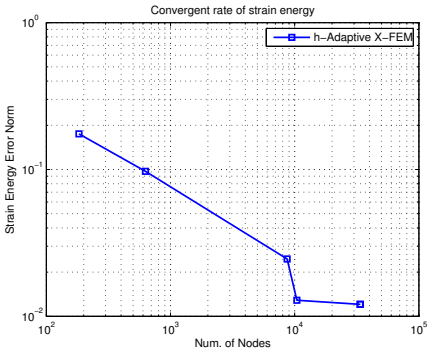

(b) Convergent rate of strain energy

Figure 8: Plot of Convergent rate of the cylinder model

spent by the optimization based on adaptive meshes is 9.353% less than optimization based on uniform meshes, and meanwhile, they have very close objective. The convergent history of objective and volume constraint is illustrated in Figure (12).

Table 2: Comparison of efficiency between optimizations of cantilever beam based on uniform and adaptive meshes respectively

Item	Iterations	Threshold	Objective	Total Time(s)	Time Saving(%)
h-Adaptive	200	3	31.3067	343.470	9.353
Uniform	200	> 128	31.5928	367.243	0

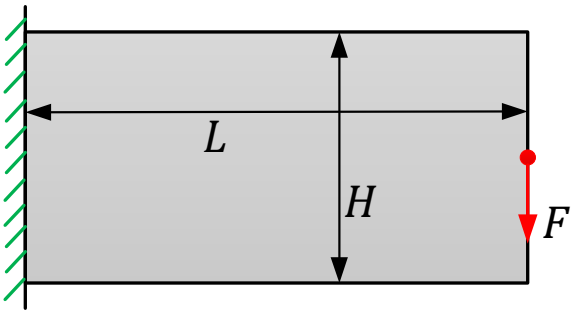

Figure 9: A cantilever beam

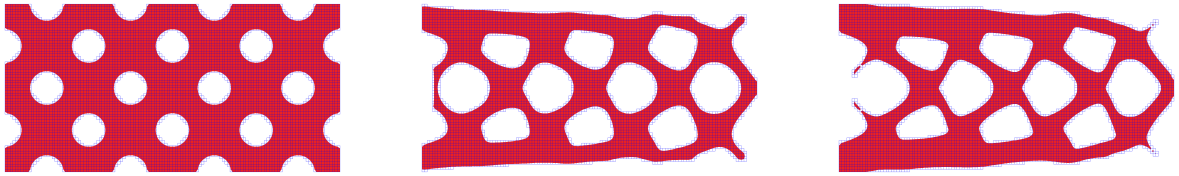

(a) Inital design (b) Step 40 (c) Step 80

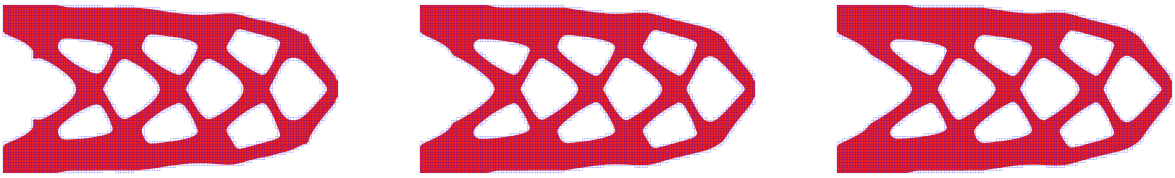

(d) Step 120 (e) Step 160 (f) Step 200

Figure 10: The intermediate results of model of uniform meshes

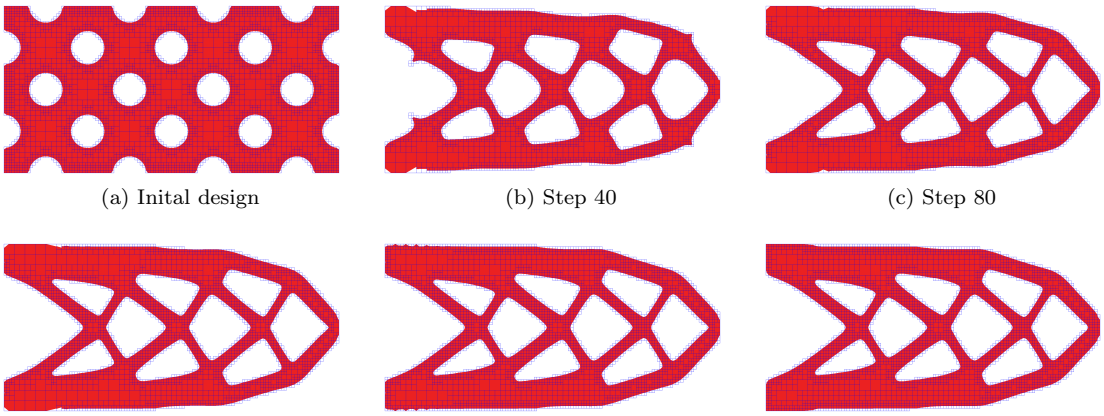

(a) Inital design (b) Step 40 (c) Step 80

(d) Step 120 (e) Step 160 (f) Step 200

Figure 11: The intermediate results of model of adaptive meshes

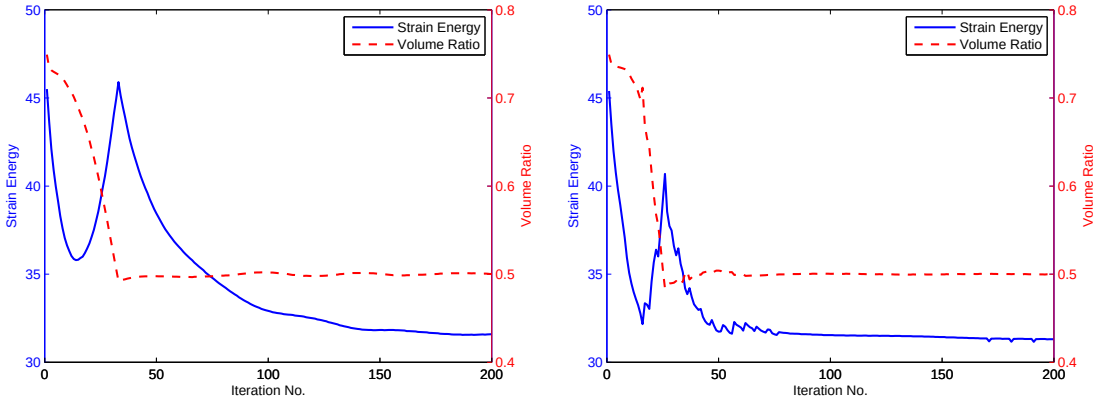

(a) Cantilever beam of uniform meshes (b) Cantilever beam of adaptive meshes

Figure 12: Convergent history of strain energy and volume ratio

6. Acknowledgements

The research work reported in this paper is sponsored in part by the Hong Kong Research Grants Council (grant CUHK 417309).

7. References

[1] T. Belytschko, S.P. Xiao, and C. Parimi, Topology optimization with implicit functions and regularization, *International Journal for Numerical Methods in Engineering*, 57, 1177-1196, 2003

[2] P. Duysinx, L.V. Miegroet, T. Jacobs, and C. Fleury, Generalized shape optimization using X-FEM and level set methods, *IUTAM Symposium on Topological Design Optimization of Structures, Machines and Materials*, 23-32, 2006

[**3**] L.V. Miegroet, T. Jacobs, and P. Duysinx, Recent developments in fixed mesh optimization with X-FEM and level set description, *7th World Congress on Structural and Multidisciplinary Optimization (WCSMO-7)*, 1947–1956, 2007

[**4**] L.V. Miegroet and P. Duysinx, 3D shape optimization with X-FEM and a level set constructive geometry approach, 8th World Congress on Structural and Multidisciplinary Optimization (WCSMO-8), 1453-1463, 2009

[**5**] L.V. Miegroet and P. Duysinx, Stress concentration minimization of 2D filets using X-FEM and level set description, *Structural and Multidisciplinary Optimization*, 33, 425-438, 2007

[**6**] D.K. Lee, A. Lipka, and E. Ramm, Nodal-based topology optimization using X-FEM and level sets, *7th World Congress on Structural and Multidisciplinary Optimization (WCSMO-7)*, 1987–1996, 2007

[**7**] P. Wei, M.Y. Wang, and X.H. Xing, A study on X-FEM in continuum structural optimization using level set model, *Computer-Aided Design*, 42, 708-719, 2010

[**8**] LI Li, Extended Finite Element Method Schemes for Structural Topology Optimization, *The Chinese University of Hong Kong*, July 2012

[**9**] Laurent Van Miegroet, Generalized Shape Optimization using XFEM and Level Set Description, *University of Liege*, July, 2012

[**10**] C. Daux, N. Moës, J. Dolbow, N. Sukumar, and T. Belytschko, Arbitrary branched and intersecting cracks with the extended finite element method, *International Journal for Numerical Methods in Engineering*, 48, 1741-1760, 2000

[**11**] Sukumar, N and Chopp, DL and Moës, Nicolas and Belytschko, T, Modeling holes and inclusions by level sets in the extended finite-element method, *Computer methods in applied mechanics and engineering*, 190(46), 6183–6200, 2001

[**12**] Ainsworth, Mark and Senior, Bill, Aspects of an adaptive¡ i¿ hp¡/i¿-finite element method: Adaptive strategy, conforming approximation and efficient solvers, *Computer Methods in Applied Mechanics and Engineering*, 150(1), 65–87, 1997

[**13**] Niekamp, Rainer and Stein, Erwin, An object-oriented approach for parallel two-and three-dimensional adaptive finite element computations, *Computers & structures*, 80(3), 317–328, 2002

[**14**] Bank, Randolph E and Sherman, Andrew H and Weiser, Alan, Some refinement algorithms and data structures for regular local mesh refinement, *Scientific Computing, Applications of Mathematics and Computing to the Physical Sciences*, 1, 3–17, 1983

[**15**] Fries, Thomas-Peter and Byfut, Andreas and Alizada, Alaskar and Cheng, Kwok Wah and Schröder, Andreas, Hanging nodes and xfem, *International Journal for Numerical Methods in Engineering*, 86, 4-5, 404–430, 2011

[**16**] Gupta, AK, A finite element for transition from a fine to a coarse grid, *International Journal for Numerical Methods in Engineering*, 12(1), 35–45, 1978

[**17**] Morton, DJ and Tyler, JM and Dorroh, JR, A new 3D finite element for adaptive h-refinement in 1-irregular meshes, *International journal for numerical methods in engineering*, 38(23), 3989–4008, 1995

[**18**] Nitsche, J, Über ein Variationsprinzip zur Lösung von Dirichlet-Problemen bei Verwendung von Teilräumen, die keinen Randbedingungen unterworfen sind, *Abhandlungen aus dem Mathematischen Seminar der Universität Hamburg*, 36(1), 9–15, 1971

[**19**] Wang, Michael Yu and Wang, Xiaoming and Guo, Dongming, A level set method for structural topology optimization, *Computer methods in applied mechanics and engineering*, 192(1), 227–246, 2003